

Geometric design of microfluidic chambers: platelet adhesion versus accumulation

Lauren D. C. Casa · David N. Ku

Published online: 28 September 2013
© Springer Science+Business Media New York 2013

Abstract Arterial, platelet-rich thrombosis depends on shear rates and integrin binding to either a collagen surface or to the growing thrombus, which are mechanistically different. In general, small microfluidic test sections may favor platelet-surface adhesion without testing for the primary mode of intra-arterial thrombosis, i.e. platelet-platelet bonding and accumulation. In the present report, the ratio of platelet-platelet to platelet-surface interactions, R , and the percentage of platelet-platelet interactions, P , are estimated using an analytical approach for circular and rectangular test sections. Results show that the test section geometry strongly affects both R and P , with test section height in low-aspect ratio channels or diameter greater than 90 μm dominated by platelet-platelet interactions ($R > 10$). Increasing rectangular test section aspect ratio decreases the required height. R increases linearly while P approaches 100 % asymptotically with increasing channel dimension. Analysis of platelet shape shows that the assumption of spherical platelets has a small effect on R compared to discoid platelets adhering flat against test section wall. However, an increase in average platelet volume resulted in a large decrease in R . Nonetheless, Monte Carlo simulations of a typical distribution of human platelet sizes show intrasubject variation in platelet size has only a 10 % net effect on R . Finally, experiments of thrombus formation show that platelet-surface lag times and platelet-platelet accumulation are similar for rectangular microfluidic test sections and round test sections when $R > 10$. The findings show that the size of a microfluidic test section should be carefully considered in studies of cell-cell accumulation versus cell-surface adhesion.

Keywords Thrombosis · Platelets · Cell adhesion · Platelet-platelet accumulation · Microfluidic design

1 Introduction

Platelet thrombosis related to myocardial infarction and stroke forms under arterial flow conditions (Cadroy et al. 1989) and is initiated by platelet interactions with extracellular matrix proteins such as collagen or fibrinogen (Savage et al. 1996, 1998) exposed by atherosclerotic plaque rupture (Falk 1983). Subsequently platelet-platelet adhesion creates the large volume of thrombus growth (Maxwell et al. 2007) leading to occlusion of flow in atherosclerotic arteries (Davies and Thomas 1984). Intravascular thrombosis of medium and large arteries is dominated by platelet-platelet interactions due to the large ratio of thrombus volume-to-surface area in the occluded region.

Microfluidic systems are designed to utilize small fluid volumes. However, the quest for miniaturization may skew the study towards platelet-surface adhesion due to the larger surface area relative to thrombus volume. Platelets adhere to extracellular matrix proteins via different molecular mechanisms than platelet-platelet binding (Ruggeri and Mendolicchio 2007). Thus, test channels that are very small may create platelet surface adhesion, while larger ones can test for platelet-platelet bonding. The question is “How small is small?” To quantify the type of platelet adhesion event within a test channel, we characterize microfluidic assays as dominated by either platelet-surface or platelet-platelet interactions. Multiple investigators have described flow assays to quantify platelet adhesion, summarized in Table 1. Some of the studies utilized surface coverage measurement techniques and short test times to isolate platelet-surface interactions. Others created a thrombus that fills a large portion or all of the test section,

L. D. C. Casa · D. N. Ku (✉)
George W. Woodruff School of Mechanical Engineering, Georgia
Institute of Technology, Atlanta, GA 30332-0405, USA
e-mail: david.ku@me.gatech.edu

Table 1 Summary of previous arterial platelet adhesion and aggregation assays

Test Section Geometry	Test Time	Endpoint	References
Cylindrical (stenosed)			
$D=2$ mm $D=1.3$ mm $D=0.9$ mm $D=4$ mm $D=300$ μ m	30 min.	Platelet deposition	(Badimon et al. 1986; Badimon and Badimon 1989; Mailhac et al. 1994)
	20 min.	Thrombus volume	(Bark et al. 2012; Ku and Flannery 2007; Para et al. 2011)
Parallel Plate			
$h=1$ mm, $w=10$ mm $\alpha=10$	5 min.	Surface coverage	(Houdijk et al. 1986; Sakariassen et al. 1983)
$h=254$ μ m, $w=0.22$ cm $\alpha=8.7$	2 min.	Thrombus volume & height	(Savage et al. 1996, 1998, 1999; Usami et al. 1993)
$h=0.1$ mm, $w=5$ mm $\alpha=50$	5 min.	Surface coverage	(Sixma et al. 1998)
$h=60$ μ m, $w=250$ μ m $\alpha=4.2$	7 min. (occlusion)	Fluorescence	(Colace et al. 2012; Maloney et al. 2010)
$h=80$ μ m, $w=100$ μ m $\alpha=1.25$	5 min.	Surface coverage	(Neeves et al. 2008)
$h=24$ μ m, $w=200$ μ m $\alpha=8.3$	1 min.	Fluorescence	(Gutierrez et al. 2008)
$h=80$ μ m, $w=300$ μ m $\alpha=3.75$	30 min. (occlusion)	Pressure drop	(Hosokawa et al. 2011)
$h=w=40$ μ m $\alpha=1$	10 min (occlusion)	Pressure drop	(Hosokawa et al. 2012)
Parallel Plate (stenosed)			
$w=5$ mm $h=0.7$ mm, $\alpha=7.1$ $h=0.28$ mm, $\alpha=17.9$ $h=0.14$ mm, $\alpha=35.7$ $h=0.08$ mm, $\alpha=62.5$	5 min.	Thrombus volume	(Barstad et al. 1994, 1995a, b; Bossavy et al. 1999; Sakariassen et al. 1990)
$h=250$ μ m, $w=750$ μ m $\alpha=3$	10 min. (occlusion)	Occlusion time & blood volume	(Li et al. 2012)

and it is unclear whether platelet-platelet or platelet-surface effects were dominant. Though the results of these studies depend on many factors including time, shear rate, and biomolecular interactions, the dominant type of platelet adhesion event, namely platelet-surface or platelet-platelet, depends on size of the test section and final thrombus volume. In future studies, it may be advantageous to design test sections to separate the effects of the different platelet adhesion mechanisms. In particular, it is of interest to determine the minimum allowable size of a microfluidic test section that still permits the observation of large-scale occlusive thrombosis in which many more platelets adhere to each other rather than to the test section walls.

The objective of the present study is to determine the dimensions and conditions for microfluidic assays that favor one type of platelet interaction over another. The ratio of platelet-platelet to platelet-surface interactions,

R , and the percent of platelet-platelet interactions, P , are estimated for circular and rectangular test section geometries. For rectangular test sections, a range of channel aspect ratios are considered: channels with all sides functionalized versus only one side functionalized, where “functionalized” refers to areas of the channel coated with an adhesive protein. The effects of platelet size and shape are also investigated, and analytical predictions are shown experimentally by comparing a rectangular microfluidic channel to a circular test section that mimics a stenotic coronary artery. Results of this analysis may be useful for the development of micro-scale assays to study either cell-cell or cell-surface bonding. Results may also be extended to characterize micro- and nano-fluidic analyses of leukocyte accumulation, three-dimensional cell culture, and colloidal fouling.

2 Methods

2.1 General analysis

In general, the **ratio**, R , of platelet-platelet to platelet-surface interactions and the **percentage**, P , of platelet-platelet interactions were defined as

$$R = \frac{N_p}{N_s}, \tag{1a}$$

$$P = \frac{N_p}{N_{tot}} \tag{1b}$$

where N_{tot} is the total number of adhered platelets, and N_s and N_p are the number of platelets adhered to the surface and to other platelets, respectively. Since in many experimental procedures, the number of platelets is difficult to measure directly, N_{tot} was approximated as

$$N_{tot} = \frac{pV}{v} \tag{2}$$

where V is the measured thrombus volume per unit length, p is the fraction of the thrombus composed of platelets, here assumed to be 80 % ($p=0.8$) (Ku and Flannery 2007), and v is the average volume of an individual platelet. The number of surface-adhered platelets, N_s , was approximated as

$$N_s = \frac{A}{a} \tag{3}$$

where A is the area of the functionalized surface supporting platelet adhesion per unit length, and a is the area occupied by an individual adhered platelet. Finally, the number of platelets adhered to other platelets, N_p , was calculated as

$$N_p = N_{tot} - N_s. \tag{4}$$

2.2 Analysis for fully occluded test sections

The effect of channel dimensions on R and P were analyzed based on the following. Two common test section geometries, circular and rectangular (Fig. 1), were considered in the present analysis. Circular cross-sections were quantified by diameter, D , and rectangular test sections were characterized by height, h , and aspect ratio, α , defined as width over height, w/h . For circular test sections, the entire inner surface was considered functionalized to support platelet adhesion. For rectangular test sections, two surface functionalization configurations were considered. First, all interior surfaces were considered functionalized. The analysis was repeated assuming only one surface, either the top or bottom, was

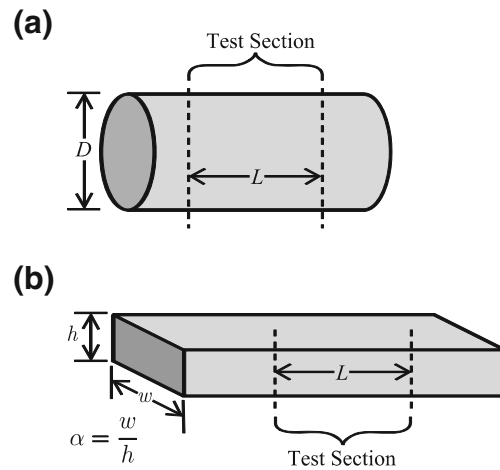


Fig. 1 Test section geometry, (a) circular, (b) rectangular

functionalized, similar to previous experiments (Barstad et al. 1994, 1995a, b; Bossavy et al. 1999; Colace et al. 2011; Gutierrez et al. 2008; Hosokawa et al. 2011; 2012; Houdijk et al. 1986; Maloney et al. 2010; Neeves et al. 2008; Sakariassen et al. 1983, 1990; Savage et al. 1996, 1998, 1999; Sixma et al. 1998). For all geometries, the analysis was performed assuming a section of arbitrary length, L , over which the surface is functionalized to support platelet adhesion.

For test sections that are fully occluded by thrombus, the thrombus volume per unit length for circular and rectangular test sections, V_C and V_R , respectively, were calculated from geometry as

$$V_C = \frac{\pi D^2}{4}, \tag{5a}$$

$$V_R = \alpha h^2 \tag{5b}$$

where α is the aspect ratio of the rectangular channel defined as width divided by height (w/h). For test sections with all surfaces functionalized to support platelet adhesion, the adhesive area per unit length for circular and rectangular test sections, A_C and A_R , respectively, were calculated from geometry as

$$A_C = \pi D, \tag{6a}$$

$$A_R = 2h(1 + \alpha). \tag{6b}$$

Substituting Eqs. 5a and 6a into Eqs. 1a, 1b–4 and simplifying gave the following for circular test sections.

$$R_C = \frac{Dpa}{4v} - 1 \tag{7a}$$

$$P_C = 1 - \frac{4v}{Dpa} \quad (7b)$$

where p is the percentage of the thrombus composed of platelets, v is the volume of an individual platelets, and a is the surface area occupied by an individual platelet. Similarly, substitution yielded the following for rectangular test sections.

$$R_R = \frac{\alpha hpa}{2v(1 + \alpha)} - 1 \quad (8a)$$

$$P_R = 1 - \frac{2v(1 + \alpha)}{\alpha hpa} \quad (8b)$$

In many experimental assays (see Table 1), a rectangular test section has been used with only the bottom or top surface functionalized to support platelet adhesion to simulate local atherosclerotic plaque rupture. In this case, the occlusive thrombus volume is identical to that given in Eq. 5b, but the area per unit length, A_B was calculated as

$$A_B = \alpha h. \quad (9)$$

Substituting again into Eqs. 1a, 1b–4 gave the following for occlusive thrombus in rectangular test with only the bottom or top surface functionalized

$$R_B = \frac{hpa}{v} - 1 \quad (10a)$$

$$P_B = 1 - \frac{v}{hpa}. \quad (10b)$$

For the present analysis, D was varied from 10 μm to 1,000 μm for circular test sections, and for rectangular test sections, h was varied from 20 μm to 1,000 μm and α from 1 to 70. Dimensions were chosen to correspond with the range of test section dimensions summarized in Table 1 as well as to investigate smaller microfluidic test sections. Channel dimensions less than 10 μm were not considered based on observations that average human platelet diameters are approximately 3.6 μm (Frojmovic and Panjwani 1976), and thus very small dimensions would allow only one or two platelets to fill the cross-section. For the initial analysis, platelets were assumed spherical with $v=6.5$ fL (Frojmovic and Panjwani 1976).

2.3 Analysis for partially-occluded test sections

Many of the studies listed in Table 1 have short experiment times such that the rectangular test section was only partially occluded. In these cases, only one surface of the test section was functionalized, so Eq. 9 is valid for the adhesive area per unit length. Either thrombus volume, $V_{R,part}$, or thrombus

thickness, m , was measured. In the case where m was measured, $V_{R,part}$ was calculated as

$$V_{R,part} = \alpha hm. \quad (11)$$

Substituting into Eqs. 1a, 1b–4 gave the following for partially occlusive thrombus in a rectangular channel.

$$R_{R,part} = \frac{map}{v} - 1 \quad (12a)$$

$$P_{R,part} = 1 - \frac{v}{map}. \quad (12b)$$

The partial occlusions mirror the fully-occluded test sections with only the one surface functionalized, and are not treated separately in Section 3, but were used to analyze the previous results shown in Table 1.

Though not applicable to the studies shown in Table 1, for completeness, partially occlusive thrombus in a circular channel has an adhesive area per unit length given by Eq. 6a and a volume per unit length, $V_{C,part}$, given by

$$V_{C,part} = \frac{\pi}{4} [D^2 - (D-m)^2]. \quad (13)$$

Substituting into Eqs. 1a, 1b–4 gave the following for partially occlusive thrombus in a circular channel.

$$R_{C,part} = \frac{pa}{4Dv} [D^2 - (D-m)^2] - 1 \quad (14a)$$

$$P_{C,part} = 1 - \frac{4Dv}{pa} [D^2 - (D-m)^2]^{-1} \quad (14b)$$

2.4 Effect of platelet shape and size

Using the analysis above, the effect of platelet size and shape were also analyzed. For spherical platelets, the diameter, d , was calculated from v using

$$d = \left(\frac{6v}{\pi} \right)^{1/3}. \quad (15)$$

The area occupied by a surface-adhered platelet was assumed to equal the maximum cross-sectional area, namely $a = \pi d^2/4$.

Discoid platelets were also analyzed, oriented such that they adhered with their major axis parallel to the surface, “flat,” or with their major axis perpendicular to the surface, “upright.” Discoid platelet volume and geometry were quantified based on Frojmovic and Milton (1982) as

$$v = \frac{\pi}{4} d^2 t + \frac{\pi}{6} t^3 + \frac{\pi^2}{8} dt^2 \quad (16)$$

where d is the diameter and t is the thickness of the platelet. An axis ratio of 0.3 was assumed (Frojmovic and Panjwani 1976), so $t=0.3d$, and Eq. 16 was solved for d with $v=6.5$ fL. For platelets adhered in the flat position, a was assumed equal to the maximum cross sectional area, $a=\pi d^2/4$, and for platelets in the upright position, a was assumed equal to the rectangular projection of the platelet, $a=td$. The effect of platelet size was also analyzed by increasing v from 6.5 to 26 fL, four times the average platelet volume and at the upper range of observed platelet volumes (Paulus 1975). Figure 2 illustrates the analyzed platelet geometries and adhesion orientations.

2.5 Particle size distribution

In vivo, platelet size varies according to a log-normal distribution with a log-mean of 1.68 fL and a log-standard deviation of 0.61 fL (Paulus 1975). To model the effect of platelet volume variation, repeated Monte Carlo simulations of platelet adhesion were performed by generating arrays of random platelet sizes according to this distribution. The array represented sequentially bound platelets within the test sections.

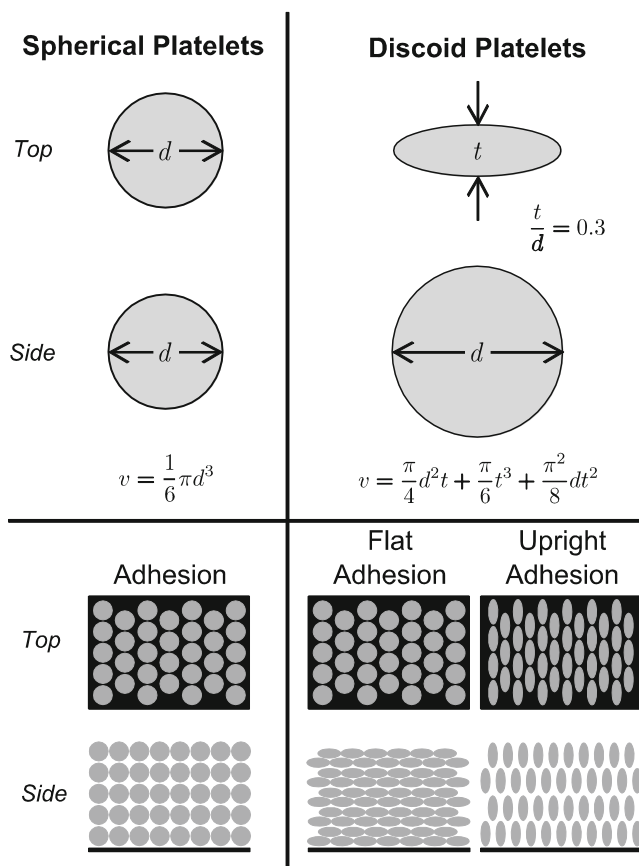


Fig. 2 Platelet and adhesion geometry. For the initial analysis, all platelets were assumed to have the same volume of 6.5 fL. For spherical platelet (*left*), the diameter, d , was 2.3 μm , and for discoid platelets (*right*), $d=2.6$ μm and the thickness, t , was 0.8 μm

Stepping through the array, the functionalized surface of the test section was assumed to be coated first by subtracting the calculated area of the platelet from the total functionalized surface area and the volume of the platelet from the total test volume. After full surface coverage, each subsequent adherent platelet volume was subtracted from the total test volume until it was completely filled. The algorithm assigned first all surface-bound and then all platelet-bound platelets. This assignment may not necessarily mimic *in vivo* or *in vitro* thrombosis, but rather was employed as a way to systematically step through the array of platelet sizes. Assigning platelet locations randomly within the test volume and then analyzing the surface- versus platelet-bound platelets does not affect the results. R and P were calculated for each simulation based on the number of platelets adhered to the surface and total number of platelets necessary to fill the test section volume. The simulations were repeated at least 4 times and continued until the standard error of the mean (standard deviation divided by the square root of the number of trials) was less than 1 % of the mean for both R and P .

2.6 Experimental demonstration of $R > 10$

To illustrate the applicability of the preceding analysis to experimental systems, a rectangular microfluidic stenotic test section was designed with $R > 10$ yielding cross-sectional dimensions of $h=70$ μm and $w=475$ μm ($\alpha=6.8$). The test section was fabricated from PDMS and plasma-bonded to a glass microscope slide using standard techniques. To support platelet adhesion, the test section was coated with fibrillar collagen Type I (Chronopar; Chronolog, Inc.; Havertown, PA) for 24 h in a warm, moist environment and rinsed with PBS prior to experimentation. Whole blood was obtained from a healthy donor under an approved IRB protocol. Blood was lightly heparinized at 3.5 USP units/mL (Para et al. 2011). Blood was perfused through the test section as a mean shear rate of 6,500 s^{-1} under a constant pressure head.

To compare microfluidic test section performance to a test section that more closely mimics coronary artery geometry, whole blood from the same donor was also perfused through a circular stenotic glass test section ($R > 10$, $D=345$ μm , 77 % stenosis), as described previously (Ku and Flannery 2007; Para et al. 2011). The test section was incubated with collagen, and the mean shear rate was matched to that of the microfluidic system. In the circular system, the discharge mass was measured using a scale.

Microscopy images of thrombus formation in each test section were recorded at 2 Hz using a high resolution CCD (Pixelfly; PCO; Kelheim, Germany) attached to a stereo microscope (Leica DM5000b; Leica Microsystems; Wetzlar, Germany and Stemi 2000-C; Carl Zeiss; Oberkochen, Germany). The images were analyzed using an automated image analysis program developed in MATLAB (R2012a;

The Mathworks, Inc.; Natick, MA). For both systems, a reference image taken prior to thrombus formation was selected and subtracted from subsequent images to highlight intensity changes resulting from the thrombus. For the microfluidic system, the total intensity in the region of interest was quantified as a surrogate for thrombus volume, which is not readily obtainable from the *en face* images. In the circular system, thrombus was identified using a user-defined threshold, and the thrombus volume was then estimated using a summation of differential volumes (Para et al. 2011).

Platelet adhesion to the collagen surface typically exhibits by a lag time before large thrombus formation. In contrast, platelet-platelet volume growth is characterized primarily by the occlusion time. The lag time, t_{lag} , and the occlusion time, t_{occ} , were quantified for both test sections. For the microfluidic system, t_{lag} was identified from the intensity versus time graph as an initial non-linear region of thrombus formation, and t_{occ} was determined by identifying the microscopy image in which flow ceased, based on cell motion. For the circular, true-sized system, t_{lag} was defined as when the thrombus volume in the region of interest exceeded 0.001 mm^3 , and t_{occ} was defined as when the discharge mass no longer changed.

3 Results

3.1 Analytical results

In circular test sections, R_C increased linearly with D (Fig. 3a), and P_C asymptotically approached 100 % (Fig. 3b). Similar results were seen for rectangular test

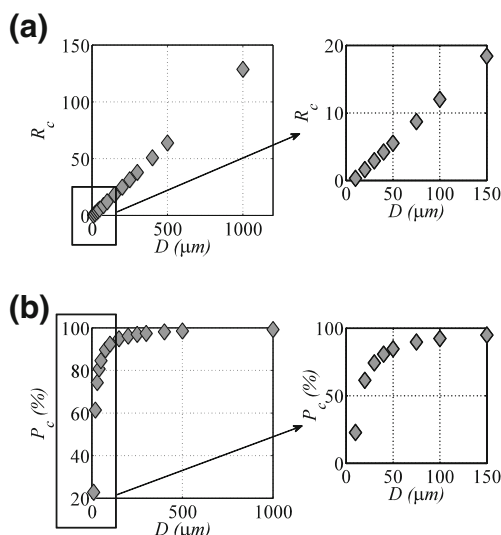


Fig. 3 Effect of circular test section size on (a) platelet-platelet to platelet-surface interaction ratio, R_C , and (b) percent platelet-platelet interactions, P_C

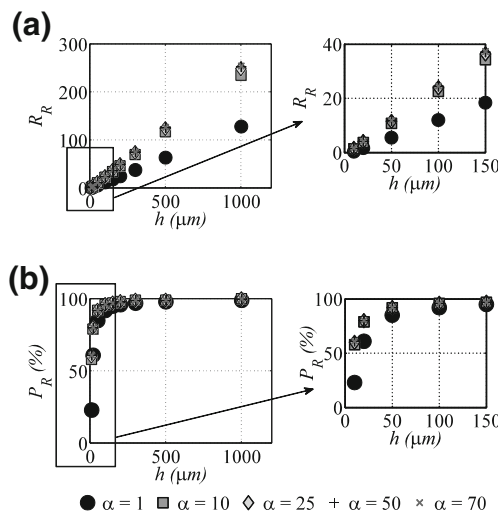


Fig. 4 Effect of rectangular test section size with all sides functionalized on (a) platelet-platelet to platelet-surface interaction ratio, R_R , and (b) percent platelet-platelet interactions, P_R

sections (Fig. 4). As α decreased in rectangular channels, the rate of increase of both R_R and P_R decreased, and thus low aspect ratio channels favor platelet-surface interactions. For rectangular channels with only one surface supporting platelet adhesion, α does not affect R_B or P_B (Fig. 5), as evident by the absence of α in Eqs. 10a and 10b. Rectangular sections with only one surface functionalized had higher R and P and thus favor platelet-platelet interactions, compared to rectangular test sections with all surfaces functionalized.

Defining $R \geq 10$ (that is, ten times as many platelet-platelet adhesion events at platelet-surface adhesion events) as a threshold for an assay dominated by platelet-platelet interactions, circular test sections meant for full occlusion during experimentation should be manufactured with $D \geq 90 \mu\text{m}$.

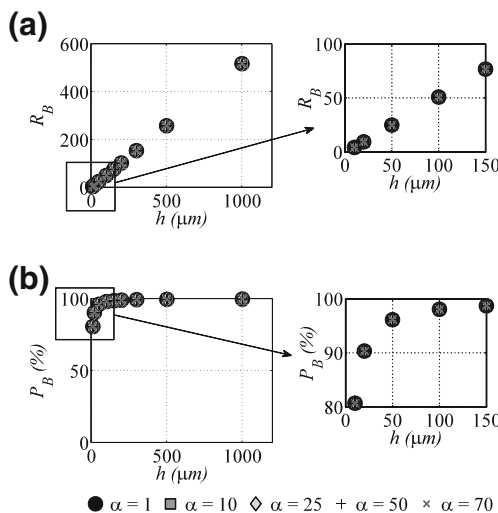


Fig. 5 Effect of rectangular test section size with single surface functionalization on (a) platelet-platelet to platelet-surface interaction ratio, R_B , and (b) percent platelet-platelet interactions, P_B

Rectangular sections with low aspect ratios and all surfaces functionalized should have $h \geq 90 \mu\text{m}$. Rectangular sections with large aspect ratios may be reduced to $h > 50 \mu\text{m}$ and still be dominated by platelet-platelet interactions. In rectangular channels with only one surface functionalized, h should be greater than $20 \mu\text{m}$ for platelet-platelet interactions to dominate thrombus formation. To isolate platelet-surface interactions ($P < 50\%$), circular channels with $D < 20 \mu\text{m}$ should be used. Alternatively, rectangular channels with only the one surface functionalized may be used to isolated platelet-surface interactions provided that thrombus thickness is limited to less than $10 \mu\text{m}$.

Discoid platelets can be oriented flat to the surface or with their major axis perpendicular to the surface (upright). Figure 6 shows the effect of platelet shape on R and P in circular channels. Similar results were obtained for rectangular channels, but are not shown for conciseness. The effect of changing platelet shape from spherical to discoid had a limited effect on R and P when platelets are oriented flat against the test section wall (Fig. 6), with discoid platelets slightly increasing R and P compared to spherical platelets. When platelets are oriented upright against the wall, R is substantially decreased compared to spherical platelets, and P is substantially decreased at small D with less effect as D increases. The larger effect of upright platelets compared to spherical platelets is due to an increase in the ratio of platelet volume to occupied surface area, v/a , from $1.4 \mu\text{m}$ for spherical platelets to $2.9 \mu\text{m}$ for upright platelets. Each surface adherent platelet occupies more volume per unit area in the upright position than in the flat or spherical position. This increases the number of platelets necessary to cover the surface without affecting the total number of platelets in the volume, thus resulting in a larger decrease in both R and P . In the case of flat platelets, v/a is slightly decreased compared

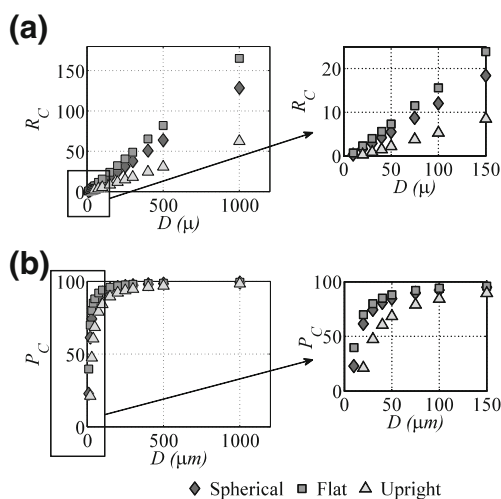


Fig. 6 Effect of platelet shape on (a) platelet-platelet to platelet-surface interaction ratio, R_C , and (b) percent platelet-platelet interactions, P_C , in circular test sections

to spherical platelets to $1.1 \mu\text{m}$, resulting in a smaller opposite effect. Given that Maxwell et al. (2006) showed that platelet morphology during translocation varies between discs adhered flat against the wall and spheres, depending on shear rate, the case of upright platelet adhesion seems unlikely under high shear. Thus, the results of platelet shape variation suggest that a simplified spherical geometric assumption yields similar results to flat platelet adhesion and is likely sufficient for design and characterization of microfluidic platelet assays.

Based on the preceding results classifying test section dimensions of $< 20 \mu\text{m}$ for predominately platelet-surface interactions, or $> 90 \mu\text{m}$ for predominately platelet-platelet interactions, the subsequent analyses were performed for test sections sizes of 20, 100, and $500 \mu\text{m}$ ($\alpha = 10$ for rectangular channels). Increasing platelet volume, v , from 6.5 to 26 fL had a large effect on R for all platelet shapes and test section geometries (Fig. 7), with R decreasing 37–174 % depending on the test section geometry and platelet shape. The percent decrease was greatest in circular channels with $D = 20 \mu\text{m}$ and for platelets in the upright orientation. In rectangular channels,

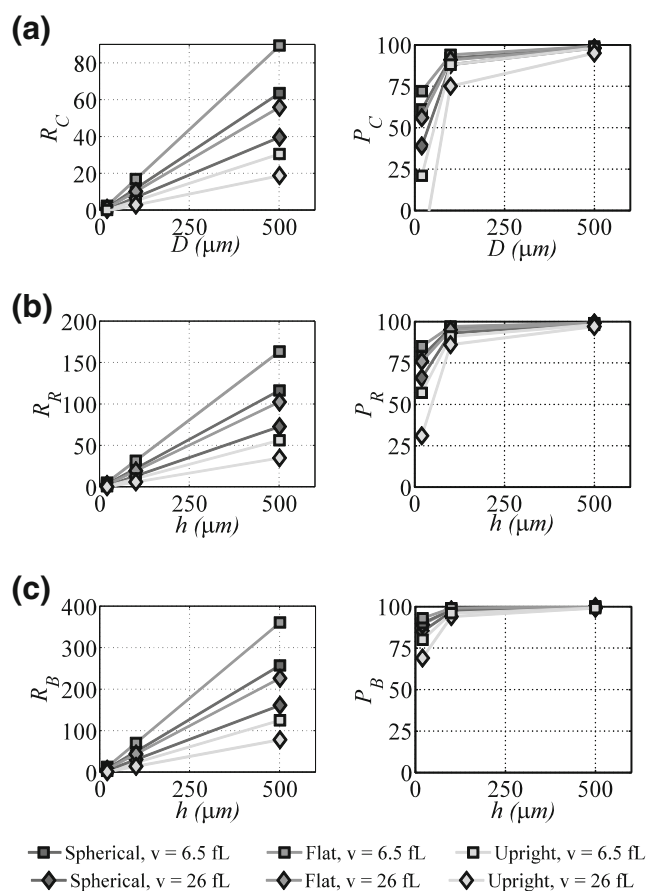


Fig. 7 Effect of platelet volume on platelet-platelet to platelet-surface interaction ratio, R (left column), and percent platelet-platelet interactions, P (right column) for (a) circular channels and rectangular channels, $\alpha = 10$, with (b) all surfaces functionalized and (c) only one surface functionalized

Table 2 Summary of Monte Carlo simulation results

D or h (μm)	Circular Test Sections			Rectangular Test Sections ($\alpha=10$)					
				All Surfaces Functionalized			Single Surface Functionalized		
	Eqs. 1a and 1b	Monte Carlo	Percent Difference	Eqs. 1a and 1b	Monte Carlo	Percent Difference	Eqs. 1a and 1b	Monte Carlo	Percent Difference
Ratio (R)									
20	1.6	1.47	-8.26 %	3.7	3.54	-4.74 %	9.4	8.85	-5.80 %
100	12.0	11.34	-5.45 %	22.6	21.68	-4.06 %	50.8	48.68	-4.42 %
500	63.8	61.77	-3.26 %	116.8	112.00	-4.27 %	258.1	249.20	-3.58 %
Percentage (P)									
20	61.4 %	59.15 %	-3.82 %	78.8 %	77.95 %	-1.06 %	90.4 %	89.83 %	-0.58 %
100	92.3 %	91.88 %	-0.44 %	95.8 %	95.59 %	-0.17 %	98.1 %	97.99 %	-0.09 %
500	98.5 %	98.41 %	-0.05 %	99.2 %	99.11 %	-0.04 %	99.6 %	99.60 %	-0.01 %

R decreased by 37.1 % to 43.6 % when discoid platelet volume was increased from 6.5 fL to 26 fL.

Monte Carlo simulations were performed for spherical platelets in each test section geometry with D or $h=20, 100,$ and $500 \mu\text{m}$ and $\alpha=10$. The results of the Monte Carlo simulation are compared with the deterministic results in Table 2. Results for R differed by less 10 % from the deterministic results, and P by less than 1 % except in the smallest test sections analyzed. Platelet variability had a greater effect in small test sections because individual platelets with smaller- or larger-than-average volumes result in a greater percent difference in the area and volume occupied compared to the test section dimensions, yielding larger differences in R and P . Still, the small effect of platelet variability on R and P suggests that the deterministic equations derived are likely sufficient for most test section characterization and design.

3.2 Experimental results

We studied the effect of R and P on observed thrombosis in two test section. Based on the geometric analysis, the circular, true-size test section yielded values of $R=43.7$ and $P=97.8$ %. Assuming all surfaces of the rectangular microfluidic test section absorbed collagen, the lower bounds of R and P were $R=14.8$ and $P=93.7$ %. However, studies have suggested that collagen is absorbed more readily onto glass than PDMS (Li 2013). Assuming only the bottom glass surface of the channels was coated with collagen, we calculate $R=35.3$ and $P=97.2$ % for our rectangular microfluidic experiments. In both cases, the test sections had the $R \geq 10$ required to observe predominantly platelet-platelet adhesion events and should be comparable.

Thrombus formation in each test section is shown in Fig. 8. In the circular, true-sized test section, thrombus formation can be seen as a narrowing of the lumen. However, in the

microfluidic system, *en face* imaging through the flowing blood shows thrombus as progressively brighter regions. Total intensity in the microfluidic test section and thrombus volume in the true-sized test section are illustrated in Fig. 9. Curves for each metric appear qualitatively similar, each with a clear initial region of minimal thrombus formation, a region of rapid, nearly linear increase in thrombus, a region of minimal thrombus growth near t_{occ} , and a sharp increase in intensity after occlusion. This final region of intensity build-up after occlusion may be due to thrombus compaction, which increased the image intensity and results in increased thrombus detection. For both test sections, t_{lag} were similar (Fig. 9a) at 113 s in the microfluidic system and 133 s in the true-sized system, a difference of only 15 %. Lag time is thought to occur from the absorption of plasma proteins, such as von Willebrand factor, that support high-shear platelet adhesion and may also account for initial activation of surface-bound

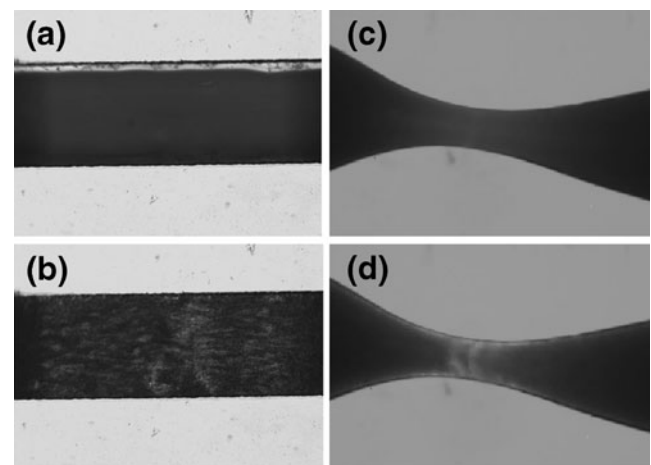


Fig. 8 Experimental test sections, (a) and (b) non-thrombosed and occluded rectangular, microfluidic test section, (c) and (d) non-thrombosed and occluded circular, true-sized test section



Fig. 9 Intensity in 70 μm rectangular test section (black) and thrombus volume in true-sized circular test section (gray) versus (a) perfusion time and (b) non-dimensional time after t_{lag} , normalized by the occlusion time

platelets. Lag time may be somewhat shorter in the microfluidic system due to the small surface area onto which proteins and platelet initially adhere. To compare the later stages of thrombus formation, the time after t_{lag} , Δt , was normalized by t_{occ} to account for differences in test section volume that must be filled with thrombus (Fig. 9b). Under this normalization, the similarities in thrombus formation between the two test sections are striking. The similarities support our analysis that large-scale platelet accumulation can be created in two test sections with very different geometry and size as long as the ratio R is above 10.

4 Discussion

Platelet thrombosis leading to arterial occlusion proceeds by platelet-surface interactions followed by platelet-platelet interactions, which are modulated by different adhesion receptors. To create these interactions *in vitro*, test section size is important. Based on the present analysis, the geometric dimensions of microfluidic assays can be used to create situations that are dominated by either type of interaction. The dominant interaction type was quantified by the ratio, R , of platelet-platelet to platelet-surface interactions and the percentage, P , of platelet-platelet interactions to total number of platelets. Analysis of platelet shape showed that the spheres may be used as a reasonable approximation for discoid platelets. Platelet size also affects adhesion, but physiologic distributions of platelet populations do not result in large errors.

Test sections with circular geometry should be designed with $D \geq 90 \mu\text{m}$ to create an assay dominated by platelet-platelet interactions ($R > 10$). For rectangular test sections, large aspect ratio channels with $h \geq 50 \mu\text{m}$ or low aspect ratio channels with $h \geq 90 \mu\text{m}$ should be used for predominately platelet-platelet interactions. Specifically, the applicability of a sufficiently large ($R > 10$) microfluidic test section for the study of occlusive arterial thrombosis in a coronary-sized vessel was demonstrated. Furthermore, experimental results may be extrapolated to conclude that in smaller test sections, thrombus formation would not progress past the lag time portion of the curve, and the distinct modes of large-scale, occlusive thrombus formation, particularly rapid platelet accumulation, may not be observed.

For predominately platelet-surface interactions ($P < 50\%$), a circular test section should be designed with $D \leq 20 \mu\text{m}$. For experiments that do not proceed to full occlusion, a rectangular test section with only the one surface functionalized may yield predominately platelet-surface interactions provided that the analysis is limited such that the thrombus thickness is less than 10 μm .

Table 3 lists the results of the present analysis applied to test section geometries from previous studies. In all experiments of this type, the dominant type of platelet interaction is determined by three factors: 1) test section geometry, 2) final thrombus volume determined either by occlusion or experimental time, and 3) the type of measurement endpoint. Several studies (Houdijk et al. 1986; Neeves et al. 2008; Sakariassen et al. 1983; Sixma et al. 1998), address platelet-surface adhesion by measurement of surface coverage only as the experimental measurement endpoint. The results of the study by Gutierrez et al. (2008) were not conducive to the present analysis, and the study was classified as a platelet-surface study due to the short test time of one minute. For these studies, R and P were calculated for thrombosis of the full test section volume. In all cases described by Houdijk et al. (1986), Neeves et al. (2008), Sakariassen et al. (1983), Sixma et al. (1998), and Gutierrez et al. (2008), the use of additional measurement endpoints combined with sufficiently long test times for large thrombus volumes would allow these test sections to be used for platelet-platelet interaction studies as well as platelet-surface interaction. For the remaining studies listed, either thrombus volume or full test section occlusion was measured, and the present analysis was applied to distinguish between studies measuring platelet-surface and platelet-platelet interactions. Except in the study by Savage et al. (1998), these studies had $R \gg 10$ and $P > 95\%$, indicating that the results of these experiments are dominated by platelet-platelet interactions and not platelet-surface interactions. In Savage et al. (1998) thrombus volume was constrained by short experiments times, thus isolating the analysis platelet-surface interactions.

In occlusive thrombus formation, which can lead to heart attack and stroke, many more platelet-platelet interactions occur compared to platelet-surface interactions, and thus it

Table 3 Application of analysis to previous high shear platelet adhesion and aggregation assays

Test Section Geometry	Ratio, R	Percentage, P	Type of Adhesion	Determining Factor	Ref.
Cylindrical (stenosed)					
$D=2$ mm	174.9	99.4 %	Platelet-Platelet	Thrombus volume	(Badimon et al. 1986; Badimon and Badimon 1989; Mailhac et al. 1994)
$D=1.3$ mm	213.4	99.5 %			
$D=0.9$ mm	78.2	98.7 %			
$D=4$ mm	73.8	98.7 %			
$D=300$ μm	41.4	97.6 %	Platelet-Platelet	Test section geometry	(Bark et al. 2012; Ku and Flannery 2007; Para et al. 2011)
Parallel Plate					
$h=1$ mm, $w=10$ mm $\alpha=10$	564.6	99.8 %	Platelet-Surface ^a	Measurement endpoint	(Houdijk et al. 1986; Sakariassen et al. 1983)
$h=254$ μm , $w=0.22$ cm $\alpha=8.7$	2.4 0.4	0.04 % 0.02 %	Platelet-Surface	Thrombus volume	(Savage et al. 1996, 1998, 1999; Usami et al. 1993)
	-0.3	-0.03 %			
$h=0.1$ mm, $w=5$ mm $\alpha=50$	55.6	98.2 %	Platelet-Surface ^a	Measurement endpoint	(Sixma et al. 1998)
$h=60$ μm , $w=250$ μm $\alpha=4.2$	32.9	97.1 %	Platelet-Platelet	Test section geometry	(Colace et al. 2012; Maloney et al. 2010)
$h=80$ μm , $w=100$ μm $\alpha=1.25$	44.2	97.8 %	Platelet-Surface ^a	Measurement endpoint	(Neeves et al. 2008)
$h=24$ μm , $w=200$ μm $\alpha=8.3$	12.6	92.6 %	Platelet-Surface ^a	Thrombus volume	(Gutierrez et al. 2008)
$h=80$ μm , $w=300$ μm $\alpha=3.75$	44.2	97.8 %	Platelet-Platelet	Test section geometry	(Hosokawa et al. 2011)
$h=w=40$ μm $\alpha=1$	21.6	95.6 %	Platelet-Platelet	Test section geometry	(Hosokawa et al. 2012)
Parallel Plate (stenosed)					
$w=5$ mm					
$h=0.7$ mm, $\alpha=7.1$	394.9	99.8 %	Platelet-Platelet	Thrombus volume	(Barstad et al. 1994, 1995a, b; Bossavy et al. 1999; Sakariassen et al. 1990)
$h=0.28$ mm, $\alpha=17.9$	157.4	99.4 %			
$h=0.14$ mm, $\alpha=35.7$	78.2	98.7 %			
$h=0.08$ mm, $\alpha=62.5$	44.2	97.8 %			
$h=250$ μm , $w=750$ μm $\alpha=3$	140.4	99.3 %	Platelet-Platelet	Test section geometry	(Li et al. 2012)

^a For studies that measured surface coverage, and therefore only platelet-surface interactions, the maximum possible R and P for the given geometry were calculated

would be advantageous to design a test section dominated by platelet-platelet interactions while minimizing the flow rate required for pathological shear rates. The present analysis yields the minimum test section dimensions that result in more platelet-platelet interactions, providing an optimum test section size for both reducing blood volume and ensuring the observation of relevant adhesion events. For clinical application of high shear platelet testing, it is desirable to reduce the required blood volume to less than 10 mL, amounts obtainable by routine phlebotomy.

The present analysis may also be applied to the adhesion and accumulation of other cells in microfluidic assays. For example, leukocyte accumulation may occur simultaneously with platelet aggregation (Hu et al. 2003; Khreiss et al. 2004), or in response to platelet microparticle release (Forlow et al.

2000) or ischemic stroke (Ritter et al. 2000). Design of microfluidic channels to isolate leukocyte-leukocyte or leukocyte-platelet adhesion by laying down a layer of platelets within a microfluidic channel may improve understanding of leukocyte accumulation in thrombus formation. Another area of application may be three-dimensional cell culture, particularly of tumor cells (Kim et al. 2007; Wu et al. 2008). The present analysis may be used to provide geometric constraints for the culture of tumor spheroids for cancer and metastasis research.

Finally, particulate-particulate and particulate-surface interactions are of critical importance to the transport of colloids in which the suspended particles may adhere to channel walls resulting in fouling and blockage. Colloidal fouling is observed in many processes, ranging from biological

applications as described here to industrial processes and devices like filtration, papermaking, heat exchangers, and oil pipelines (Adamczyk et al. 1995). Indeed, the mitigation of colloidal fouling is of perhaps greater importance in microfluidic systems where relatively small volumes of particle deposits may result in channel blockage (Mustin and Stoeber 2010). The analysis described in the present work may be applied to design microfluidic channels to investigate a multitude of fouling processes by separating the mechanisms of particulate-surface and particulate-particulate deposition and adhesion. For a relevant application, the algebraic equations presented may be applied by specifying the correct particle characteristics, namely a and v , proper deposition composition described by p , and applicable channel geometry V and A .

The present analysis of platelet accumulation has several limitations. For a given analysis condition, all platelets were assumed to have the same shape and adhere in the same orientation though in physical experiments, platelet shape and adhesion orientation may vary. Additionally, only the extremes of platelet adhesion orientation were analyzed. Cell and clot deformability and mechanics were not modeled. Coagulation and fibrin formation was not considered in the present analysis, nor were the possible effects of other clotting proteins, such as von Willebrand factor, considered. Incorporation of erythrocytes in the thrombus was not modeled nor was the adhesion of leukocytes considered. The presence of other clot constituents were accounted for by including the percent of the thrombus composed of platelets, p , in the analysis. Additionally, the present analysis does not account for the effects of hemodynamics environment, platelet activation, coagulation, biomolecular interactions, or time dependence. Rather, the present study characterizes microfluidic channels based on the type of platelet interactions, regardless of the underlying mechanisms. This type of characterization may aid in classifying previous experimental results based on platelet interaction type and may be used in the design of future microfluidic flow assays to isolate the interaction of interest.

5 Conclusion

Geometric analysis of thrombus formation in microfluidic test sections showed that test section size and thrombus volume strongly affect the proportion of platelet-platelet and platelet-surface interactions in platelet adhesion and aggregation assays. Though platelet size and shape affect platelet-platelet to platelet-surface interaction ratio and percent platelet-platelet interaction, comparison of likely platelet adhesion orientations and Monte Carlo simulation of normal human platelet size distribution suggests that quantitative algebraic relationships and a spherical platelet shape assumption are sufficient to

classify platelet aggregation studies as either dominated by platelet-platelet or platelet surface interactions. The relationships obtained from the present analysis may be used to design microfluidic test sections to separately investigate platelet-surface adhesion and platelet-platelet accumulation. In square (low aspect ratio) and round test sections, a height or diameter of 90 μm is necessary for channel occlusion to be dominated by platelet-platelet interactions ($R > 10$). The required height for $R > 10$ may be decreased to 50 μm for rectangular aspect ratios ≥ 10 . Analytical results were supported by experiments comparing two test sections of different sizes and shapes, but both with $R > 10$. The derived equations may be extended to microfluidic and nanofluidic test section design for other types of cell adhesion and aggregation, three-dimensional cell culture, and colloidal fouling applications.

Acknowledgments LDCC was supported by DoD, Air Force Office of Scientific Research, National Defense Science and Engineering Graduate (NDSEG) Fellowship, 32 CFR 168a.

References

- Z. Adamczyk, B. Siwek, L. Szyk, J. Colloid Interface Sci. **174**, 130 (1995)
- L. Badimon, J.J. Badimon, J. Clin. Invest. **84**, 1134 (1989)
- J.J. Badimon, L. Badimon, A. Galvez, J. Chesebro, V. Fuster, Arterioscler. Thromb. Vasc. Biol. **6**, 312 (1986)
- D. Bark, A. Para, D. Ku, Biotechnol. Bioeng. **109**, 2642 (2012)
- R.M. Barstad, H. Roald, Y. Cui, V. Turitto, K. Sakariassen, Arterioscler. Thromb. Vasc. Biol. **14**, 1984 (1994)
- R.M. Barstad, M.J.A.G. Hamers, R.W. Stephens, K. Sakariassen, Blood **86**, 212 (1995a)
- R.M. Barstad, H. Roald, L.B. Petersen, K. Stokke, P. Kierulf, K. Sakariassen, Blood Coagul. Fibrinolysis **6**, 372 (1995b)
- J.P. Bossavy, K.S. Sakariassen, C. Thalamas, B. Boneu, Y. Cadroy, Arterioscler. Thromb. Vasc. Biol. **19**, 2269 (1999)
- Y. Cadroy, T.A. Horbett, S. Hanson, J. Lab. Clin. Med. **113**, 436 (1989)
- T. Colace, J. Jobson, S.L. Diamond, Bioconjug. Chem. **22**, 2104 (2011)
- T. Colace, R. Muthard, S.L. Diamond, Arterioscler. Thromb. Vasc. Biol. **32**, 1466 (2012)
- M.J. Davies, A. Thomas, N. Engl. J. Med. **310**, 1137 (1984)
- E. Falk, Br. Heart J. **50**, 127 (1983)
- S. Forlow, R.P. McEver, M. Nollert, Blood **95**, 1317 (2000)
- M. Frojmovic, J. Milton, Physiol. Rev. **62**, 185 (1982)
- M. Frojmovic, R. Panjwani, Biophys. J. **16**, 1071 (1976)
- E. Gutierrez, B.G. Petrich, S.J. Shattil, M.H. Ginsberg, A. Groisman, A. Kasirer-Friede, Lab Chip **8**, 1486 (2008)
- K. Hosokawa, T. Ohnishi, T. Kondo, M. Fukasawa, T. Koide, I. Maruyama, K.A. Tanaka, J. Thromb. Haemost. JTH **9**, 2029 (2011)
- K. Hosokawa, T. Ohnishi, M. Fukasawa, T. Kondo, H. Sameshima, T. Koide, K.A. Tanaka, I. Maruyama, Microvasc. Res. **83**, 154 (2012)
- W.P. Houdijk, P.G. de Groot, P.F. Nieuvelstein, K.S. Sakariassen, J.J. Sixma, Arterioscler. Thromb. Vasc. Biol. **6**, 24 (1986)
- H. Hu, D. Varon, P. Hjemdahl, N. Savion, S. Schulman, N. Li, Thromb. Haemost. **90**, 679 (2003)
- T. Khreiss, L. Jozsef, L.A. Potempa, J.G. Filep, Circulation **110**, 2713 (2004)
- M.S. Kim, J.H. Yeon, J.K. Park, Biomed. Microdevices **9**, 25 (2007)

- D.N. Ku, C.J. Flannery, *Biorheology* **44**, 273 (2007)
- M. Li, D. Ku, C. Forest, *Lab Chip* **12**, 1355 (2012)
- M. Li, *Microfluidic System for Thrombosis under Multiple Shear Rates and Platelet Therapies*. PhD thesis, Georgia Institute of Technology, (2013)
- A. Mailhac, J. Badimon, J. Fallon, A. Fernandez-Ortiz, B. Meyer, J. Chesebro, V. Fuster, L. Badimon, *Circulation* **90**, 988 (1994)
- S.F. Maloney, L. Brass, S.L. Diamond, *Integr. Biol.* **2**, 153 (2010)
- M.J. Maxwell, S.M. Dopheide, S.J. Turner, S.P. Jackson, *Arterioscler. Thromb. Vasc. Biol.* **26**, 663 (2006)
- M.J. Maxwell, E. Westein, W.S. Nesbitt, S. Giuliano, S.M. Dopheide and S.P. Jackson, *Blood*, **109**, 566 (2007)
- B. Mustin, B. Stoeber, *Microfluid. Nanofluid.* **9**, 905 (2010)
- K. Neeves, S. Maloney, K. Fong, A. Schmaier, M. Kahn, L. Brass, S.L. Diamond, *J. Thromb. Haemost.* **6**, 2193 (2008)
- A. Para, D. Bark, A. Lin, D. Ku, *Ann. Biomed. Eng.* **39**, 1961 (2011)
- J. Paulus, *Blood* **46**, 321 (1975)
- L.S. Ritter, J.A. Orozco, B.M. Coull, P.F. McDonagh, W.I. Rosenblum, *Stroke* **31**, 1153 (2000)
- Z.M. Ruggeri, G.L. Mendolicchio, *Circ. Res.* **100**, 1673 (2007)
- K.S. Sakariassen, P. Aarts, P.G. De Groot, *J. Lab. Clin. Med.* **102**, 522 (1983)
- K.S. Sakariassen, R. Joss, R. Muggli, H. Kuhn, T.B. Tschopp, H. Sage, H.R. Baumgartner, *Arterioscler. Thromb. Vasc. Biol.* **10**, 276 (1990)
- B. Savage, E. Saldivar, Z.M. Ruggeri, *Cell* **84**, 289 (1996)
- B. Savage, F. Almus-Jacobs, Z.M. Ruggeri, *Cell* **94**, 657 (1998)
- B. Savage, D. Ginsberg, Z.M. Ruggeri, *Blood* **94**, 2704 (1999)
- J. Sixma, P.G. de Groot, H. van Zanten, M. Ijsseldijk, *Thromb. Res.* **92**, S43 (1998)
- S. Usami, H.-H. Chen, Y. Zhao, S. Chien, R. Skalak, *Ann. Biomed. Eng.* **21**, 77 (1993)
- L.Y. Wu, D. Di Carlo, L.P. Lee, *Biomed. Microdevices* **10**, 197 (2008)